Soft Matter

Retardation of Reaction Kinetics of Polymers due to Entanglement in Post-Gel Stage in Multi-Chain Slip-Spring Simulations

Journal:	*Soft Matter*
Manuscript ID	SM-ART-04-2019-000681.R1
Article Type:	Paper
Date Submitted by the Author:	20-May-2019
Complete List of Authors:	Masubuchi, Yuichi; Nagoya University, Department of Materials Physics Uneyama, Takashi; Nagoya University, Department of Materials Physics

Retardation of Reaction Kinetics of Polymers due to Entanglement in Post-Gel Stage in Multi-Chain Slip-Spring Simulations

*Yuichi Masubuchi[1] and Takashi Uneyama[2]

[1]Department of Materials Physics,

[2] Center of Computational Science,

Nagoya University, Nagoya 4648603, JAPAN.

*To whom correspondence should be addressed

mas@mp.pse.nagoya-u.ac.jp

ABSTRACT

Although the reaction kinetics of network formation for polymers has been extensively investigated, the role of entanglement between polymers has not been fully elucidated yet. In this study, we discuss the effect of entanglement via the multi-chain slip-spring simulations, in which Rouse chains are dispersed in space and connected by slip-springs that mimic the entanglement. For the stoichiometric conditions for the systems containing pre-polymers and cross-linkers, the simulations without slip-springs exhibited the reaction kinetics that is consistent with the earlier mean-field theory. Meanwhile, the inclusion of slip-springs to the system retards the reaction in the post-gel stage after the percolation of the system. According to the analysis for the network structure, the reaction in the post-gel stage is dominated by the tethered chains. The entanglement indirectly retards the reaction kinetics through the suppression of tethered chain dynamics.

Keywords

gelation, polymerization, cross-linking, polymer dynamics, coarse-grained molecular simulation

INTRODUCTION

Lots of studies have been attempted on the kinetics of network formation for polymers such as the gelation, cross-linking polymerization and thermosetting[1]. According to the mean-field theory[2,3], in the stoichiometric condition of a mixture of pre-polymers and cross-linkers, time development of the concentration of the unreacted sites $[R]$ is written as $[R] = [R]_0/(1 + 2k[R]_0 t)$, where $[R]_0$ is the initial concentration, and k is the reaction rate constant. This relation implies a power-law behavior $[R] \sim t^{-1}$ in the long-time range if k is steady. However, for most of the cases, the apparent reaction rate decreases with time because the mobility of reactants decreases with an increase of the molecular weight[4,5]. For example, in an experiment[6] for the UV curing of trimethylolpropane tris(2-mercaptoacetate) and trimethylolpropane diallyl ether, the number of unreacted sites decays with time by a power-law manner, but the exponent is -3/4 rather than -1. Similar retarded reaction kinetics has also been reported for molecular simulations[7–10]. For the gelation of a bead-spring model in molecular dynamics simulations, Grest et al.[7] reported a power-law decay for the number of unreacted sites with the exponent of -1/2. For this phenomenon, so-called auto-acceleration effect, gel-effect or Trommsdorff-Norrish effect, theoretical description for the reaction rate constant has been attempted[1]. The models have been constructed from several different bases, such as the change of reaction distance[11,12], the change of free volume of the medium[13,14], and the change of diffusion constant of the reactant[15–18].

Although an intuitive explanation for the slow reaction is the entanglement between polymers, its effect on the reaction kinetics has not been fully elucidated yet. Among the theories mentioned above, the effect of entanglement has been considered through the molecular weight dependence of the diffusion constant. Russell[16] proposed such an approach, in which the molecular weight dependence of the diffusion coefficient changes at a certain critical molecular weight, in an analogy of the onset of entanglement. Buback et al[18] introduced a similar idea as well. These theories can reproduce experimental data quantitatively, implying that the entanglement plays a role in the reaction kinetics. However, discussion for the effect of entanglement is not straightforward in the

fitting for several parameters. O'Neil et al[19] have experimentally shown that the onset of the retarded reaction is unrelated to the emergence of entanglement. They demonstrated for some entangled systems that the retardation does not occur in the early stage of the reaction. Meanwhile, they also stated that the reaction kinetics might be affected by the entanglements in the late stage.

In this study, we discuss the contribution of entanglements in the reaction kinetics of polymer gelation via cross-linking reactions. To discriminate the effects of entanglement from the excluded volume effect, we utilized the multi-chain slip-spring model, in which the entanglement effect is considered between phantom chains via the virtual springs[20]. We extended the model to gelation by introducing an end-link reaction to perform the simulations for stoichiometric mixtures containing pre-polymers and linkers. After sufficient equilibration without the reaction, the kinetics of network formation was observed. The results showed that the entanglement induces a retarded reaction even without glassy contributions in the post-gel stage. Details are shown below.

MODEL AND SIMULATIONS

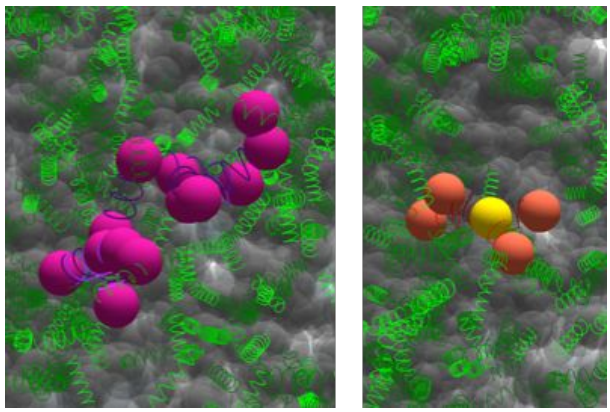

Figure 1 Typical snapshots for pre-polymer (left) and linker (right). Slip-springs are shown in green. Beads for pre-polymer segments, reactive ends, branch point, and surrounding molecules are shown in violet, red, yellow and gray.

The multi-chain slip-spring (MCSS) simulations were performed with the extension to the end-linking reaction for the network formation. In the MCSS model[20], the dynamics of bead-spring

chains without inter-beads interactions are considered. The entanglement effect is introduced by the slip-springs that temporarily connect the chains. Figure 1 left panel shows a typical snapshot for a linear polymer in the simulation. For the melts of linear[20–22] and branch polymers[23], MCSS model is capable of reproducing the diffusion and the viscoelastic relaxations with much less computational costs than the conventional Kremer-Grest[24] type simulations.

In this specific study, cross-linkers that chemically connect the pre-polymers are introduced. Figure 1 right panel shows the snapshot of a cross-linker that is a small star-branch polymer with four diverging arms from the branch point. For the bonds between beads in the pre-polymers and the cross-linkers, a linear spring force is considered with the spring constant of $3k_{\mathrm{B}}T/a^2$, where a is the average bond length. With a certain interval, the reaction is attempted for all the unreacted ends of linker molecules with the following procedure. First, an unreacted end of pre-polymer is randomly chosen from the surroundings within a specific reaction distance r_{r} from the test end of linker. (Note that r_{r} is different from the cut-off distance for the creation of slip-springs r_{c}.) Second, if an unreacted site is found, the reaction between the linker and the polymer end takes place with a reaction rate k_{r}, and a bond is formed between the beads. For the generated bonds, the spring constant is the same as that for the pre-polymers and the linkers. The bond formation is irreversible in this specific study. The heat of reaction is not considered, and the temperature is homogeneous, although the effects on the network homogeneity have been reported earlier[25]. The number ratio of the reaction sites on the cross-linkers to those on the pre-polymers is stoichiometric. It is fair to note that Megariotis et al.[26] have developed a similar extension of the slip-spring model, in parallel to, but earlier than our study. Although they reported the viscoelastic relaxation of the network after the gelation, they did not report the kinetics.

The reaction simulations were made after sufficient equilibration without reaction. For each condition, eight independent simulation runs were performed from different initial configurations for statistics. The simulations without slip-springs were also performed for comparison. Unit of length, energy, and time are the average bond length a, the thermal energy $k_{\mathrm{B}}T$, and the diffusion time for

a single bead $\zeta a^2/k_{\mathrm{B}}T$, respectively. Here, ζ is the friction coefficient of the bead. The simulation parameters were fixed, as mentioned below, unless stated. The bead number per chain for the pre-polymer N_{p} was 20, the number of pre-polymers M_{p} was 800, the linker functionality f_{L} was 4, the bead number on the linker arm N_{La} was unity, the number of linkers M_{L} was 400, and the reaction rate k_{r} was 0.1. The bead density was fixed at 4, and the slip-spring density was ca. 0.78. The cut-off distance for the creation of slip-spring was $r_{\mathrm{c}} = 1.29$. These values give the average bead number between consecutive anchoring along the chain $N_{\mathrm{e}}^{\mathrm{ss}}$ as 2.4. The numerical integration scheme employed for this study was the Verlet algorism, and the timestep used was 0.06. Periodic boundary conditions were used, and the reaction distance r_{r} was 0.5. The effects of the system size and the reaction distance shall be discussed in the Appendix.

RESULTS

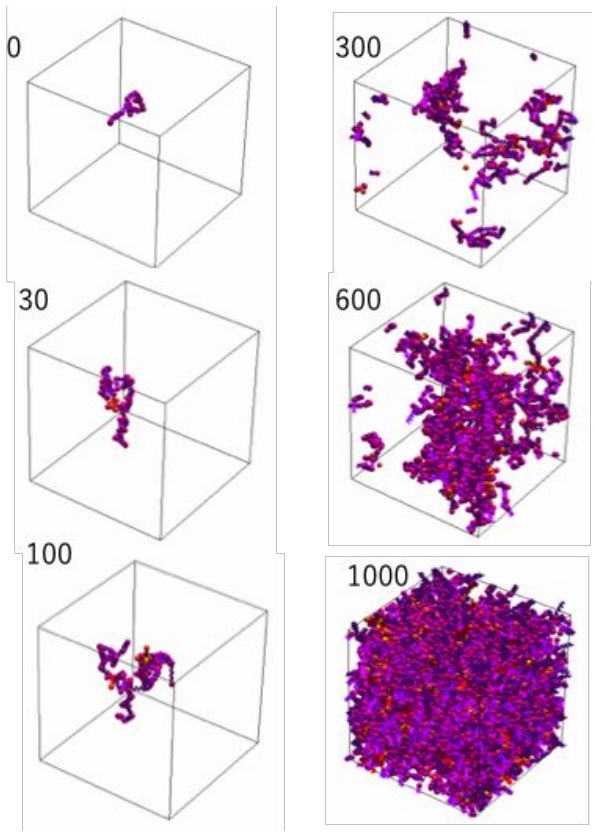

Figure 2 Snapshots of the largest cluster in the system during the reaction. The numbers indicate the simulation time from the initiation of the reaction.

Figure 2 shows typical snapshots during the reaction. The largest cluster in the system is shown here. As expected, the network growth took place by consuming the pre-polymers and the linkers owing to the end linking reaction. For this specific case (with $k_r = 0.1$), the percolation occurred around $t \sim 500$, and all the pre-polymers were attached to the network by $t \sim 1000$.

Figure 3 shows the spatial distribution of linkers (b), polymers (c), and slip-springs (d) in the snapshot (a) taken at $t = 1000$. No specific inhomogeneity was observed for all the components, irrespective of the inclusion of slip-springs.

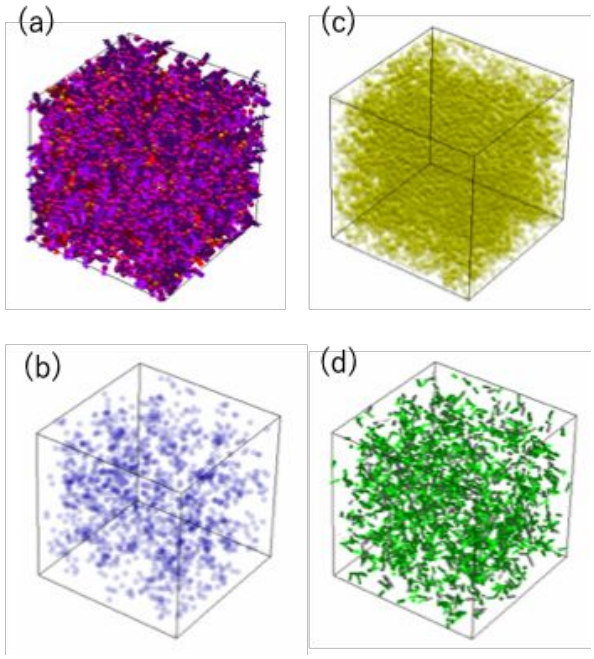

Figure 3 Spatial distribution of linkers (b), polymers (c), and slip-springs (d) for the snapshot of the entire system taken at $t = 1000$ shown in (a).

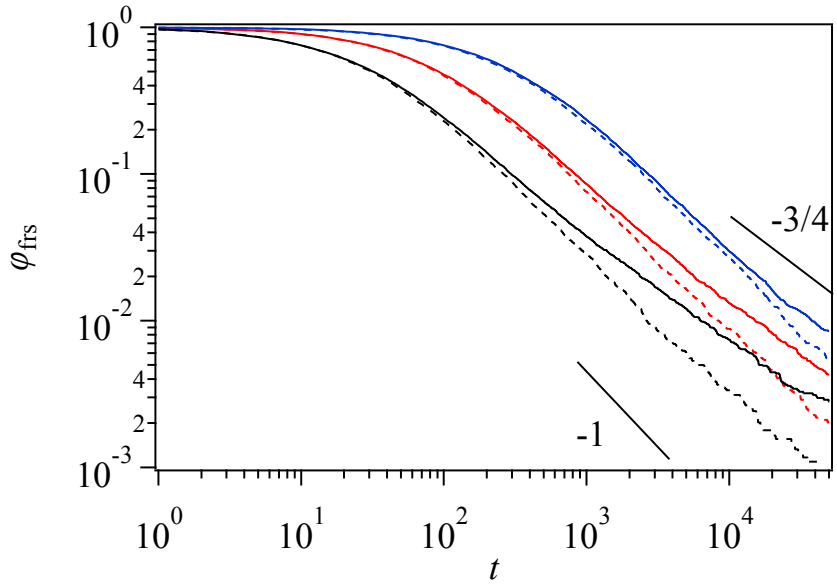

Figure 4 Time development of the number fractions of free reaction sites φ_{frs} for $k_r =$ 0.3, 0.1, and 0.03, shown in black, red, and blue, respectively. Solid and dotted curves are for the simulations with and without slip-springs, respectively. Solid lines show power-law decays with the exponent of -1 and -3/4.

Figure 4 shows the time development of the fraction of free reaction sites φ_{frs} in the simulations with and without the inclusion of slip-springs for various k_r. For the simulations without slip-springs, φ_{frs} shows a power-law decay with the exponent of -1 (see dotted curves). This result is entirely consistent with the earlier mean-field theories[2,3], and it is because the friction of the Rouse beads is kept constant. In other words, viscosity increase of the medium due to the gelation is neglected in the present simulations. For the simulations with slip-springs, φ_{frs} coincides with that without slip-springs before the percolation (see Fig 2 for $k_r = 0.1$). Although an accurate determination of the percolation is difficult in the simulations with the periodic boundary condition, the φ_{frs} value at the gelation calculated from the Flory-Stockmayer theory[27,28] is ca. 0.42, and the effect of slip-spring is not seen when φ_{frs} is larger than this value. After the percolation, (post-gel regime), φ_{frs} exhibits a delay from the unentangled case. This result is consistent with the experiment by O'Neil et al[19], who reported that the entanglement does not affect the reaction kinetics

in the early stage. In the post-gel regime, a power-law decay of φ_{frs} is observed. The exponent is larger than -1 and close to -3/4, which coincides with the result of bead-spring simulations for dilute systems[8] and the experiment for UV curing of thiol-ene polymers[6].

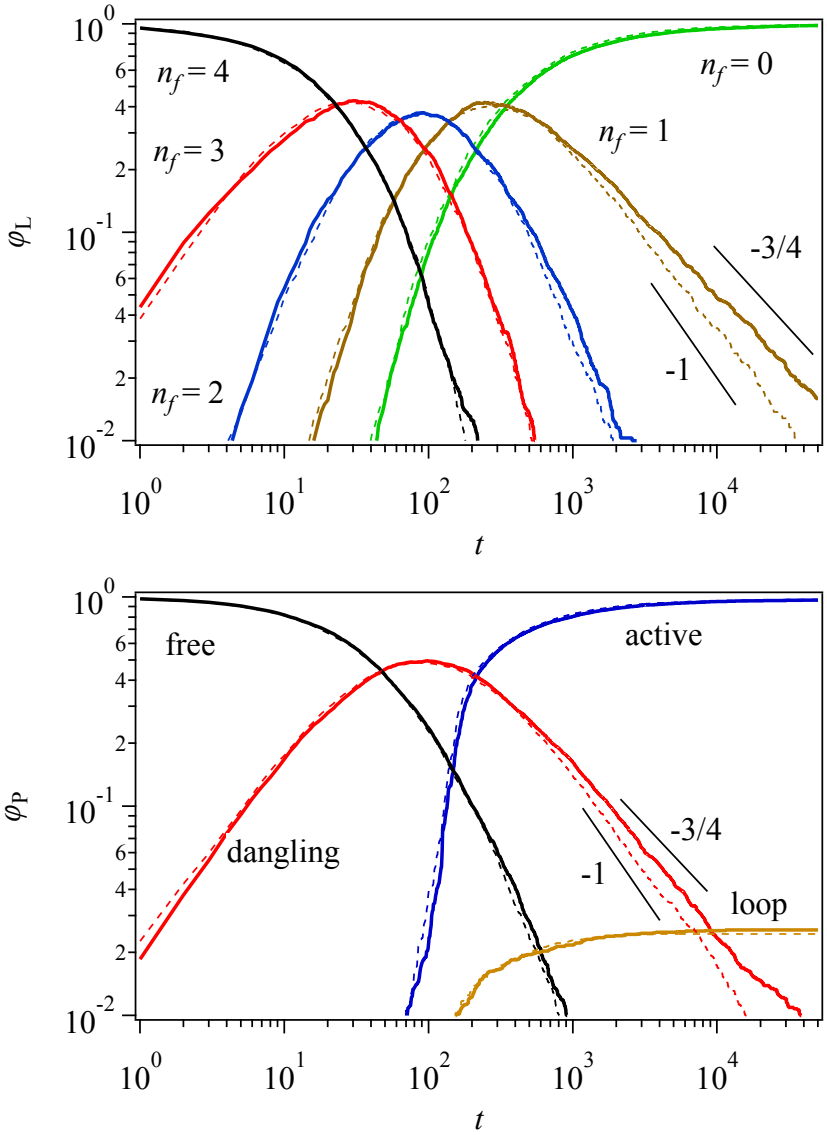

Figure 5 (Top) Time development of number fractions of linker molecules φ_{L} with various unreacted site numbers n_f, which is 4 (black), 3 (red), 2 (blue), 1 (yellow), and 0 (green). (Bottom) Time development of number fractions of pre-polymer chains φ_{P} in various topological configurations consisting of free (black), dangling (red), loop (yellow) and active (blue) chains. Broken curves are the results without slip-springs. Solid lines indicate the slope of -1 and -3/4.

Figure 5 top panel shows the time development of the number fractions of linker molecules

φ_{L} with various unreacted site numbers n_f. Namely, $n_f = 4$ corresponds to the fraction of the free linker molecules that are unconnected to any pre-polymer, whereas $n_f = 0$ is for those having no free reaction site. At the initiation of the reaction, all the reaction sites are free, and all the linkers are $n_f = 4$. As the reaction proceeds and the reaction sites are consumed, the linkers with smaller n_f values appear. Because of the stoichiometry, most of the linkers change into $n_f = 0$ at the end of the simulation, and the fraction of partly reacted linkers decays to zero. For such a reaction behavior, φ_{L} for $n_f = 4$ and 3 (black and red curves) do not exhibit the effect of slip-springs, and the curves with and without slip-springs (solid and broken curves) virtually overlap with each other. Meanwhile, φ_{L} for $n_f = 2$ and 1 (blue and yellow curves) exhibit a delayed reaction. In particular, for $n_f = 1$, the power-law decay with the exponent of -3/4 is observed for the case with slip-springs in harmony with φ_{frs}. The delayed reaction is also reflected for $n_f = 0$, although it is not seen in the logarithmic plot. This result implies that the delayed reaction is not due to the free linker diffusion, but induced by the polymers.

Figure 5 bottom panel shows the time-development of the number fractions of the pre-polymers φ_{P} with various topological configurations. As expected, the number of free-polymers (black curve) monotonically decreases with time. The consumption of free-polymers naturally leads to an increase of the chains for which the ends are connected to the linkers. The dangling chains (red curve) are one of such reacted configurations, and one of its ends is attached to a linker. The number fraction of this class shows a growth followed by decay due to the reaction of the other end. The polymers for which both ends are connected to linkers are discriminated according to the configuration into loop chains and active chains. The loop chains are the polymers for which both ends are attached to the same linker molecule, whereas the active chains have the end segments connected to different linkers. For both chains, the number fraction monotonically increases with time. The reaction kinetics shown here is similar to that reported in the earlier studies for full-atomistic simulations of epoxy resins[29]. Concerning the effect of slip-springs, it appears for the consumption of dangling chains (red curve). Namely, in the long-time range, a power-law decay is

observed, and the power-law exponent is -1 without the entanglement, whereas it is close to -3/4 with the entanglement. In comparison to the linker kinetics shown in the top panel, the delayed reaction for the dangling chains correlates with the consumptions of linker molecules with $n_f = 2$ and 1. Indeed, the retarded reaction for the dangling chains is observed in the time range of $t \geq 1000$, in which the linkers with large n_f are not seen. The difference in the decay of dangling chains must appear as a difference in the number of active chains. However, the difference is not visible in the logarithmic plot.

From the observations above, a scenario for the delayed reaction is suggested as follows. In the short time range before the network percolation, the reaction is dominated by the linker diffusion, for which the entanglement has virtually no effect. After the consumption of free linkers and the network percolation, the reaction is governed by the chain motion. In this post-gel stage, the dangling chains seek unreacted linker sites that are already embedded in the network. Such a motion of dangling chain is similar to the arm dynamics of branch polymers[30,31], and thus, the entanglement induces the retarded reaction.

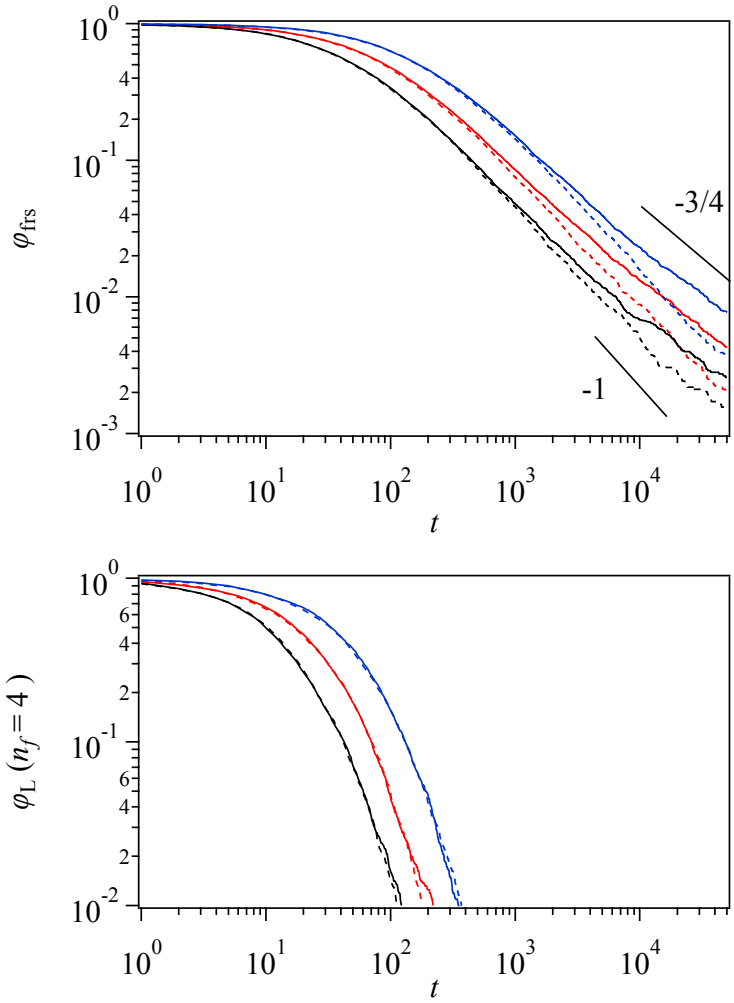

Figure 6 Time development of number fraction of free reaction sites $\varphi_{\rm frs}$ (top) and number fraction of free-linkers with $n_f = 4$ (bottom) for $N_{\rm P} =$ 10 (black), 20 (red) and 40 (blue). Solid and broken curves are for the simulations with and without slip-springs, respectively. Solid lines in the top panel show power-law decays with the exponent of -1 and -3/4.

Figure 6 top panel shows $\varphi_{\rm frs}$ for various pre-polymer lengths $N_{\rm p}$. Reflecting the slower diffusion of polymers, the longer the pre-polymer is, the slower the reaction becomes. For all the examined cases, the retarded reaction is observed for the entangled cases, and the power-law exponent is ca. -3/4. The entangled results deviate from the non-entangled ones after the consumption of free-linker molecules, as seen in the bottom panel in Fig 6, which shows the fraction of $n_f = 4$ linkers with time. This feature is consistent with the scenario mentioned above.

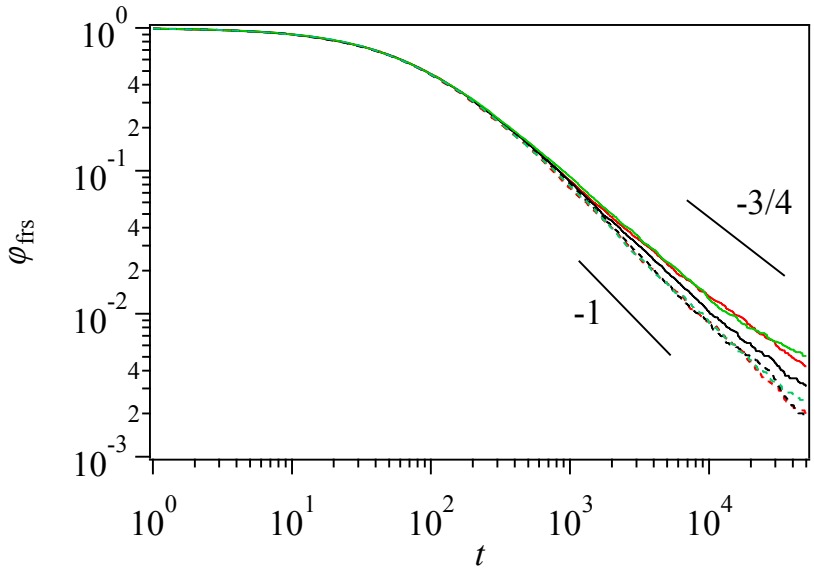

Figure 7 Time development of number fraction of free reaction sites φ_{frs} for various linker functionalities f_{L}= 3 (black), 4 (red), and 5 (green). Solid and broken curves are for the simulations with and without slip-springs, respectively. Solid lines show power-law decays with the exponent of -1 and -3/4.

Figure 7 shows φ_{frs} for various linker functionality f_{L}. Note that the stoichiometry is retained for all the examined conditions. Namely, the number of pre-polymers and the linkers are chosen at 900 and 600 for $f_{\mathrm{L}} = 3$, 800 and 400 for $f_{\mathrm{L}} = 4$, and 800 and 320 for $f_{\mathrm{L}} = 5$, respectively. Without the inclusion of slip-springs, f_{L} does not affect the reaction kinetics as demonstrated by the broken curves that overlap with each other. For the cases with slip-springs, the retarded reaction is seen for all the examined f_{L}. The onset time of the retardation becomes slightly earlier for larger f_{L}. This f_{L}-dependence of the reaction is due to the difference in the consumption speed of the free linkers, which are rapidly consumed for large f_{L} cases. The f_{L} dependence of the reaction might also imply a correlation between the unreacted polymer chains. The power-law exponent seems sensitive to f_{L} as it increases with increasing f_{L}, although the results for $f_{\mathrm{L}} = 4$ and 5 cannot be discriminated in the presented data.

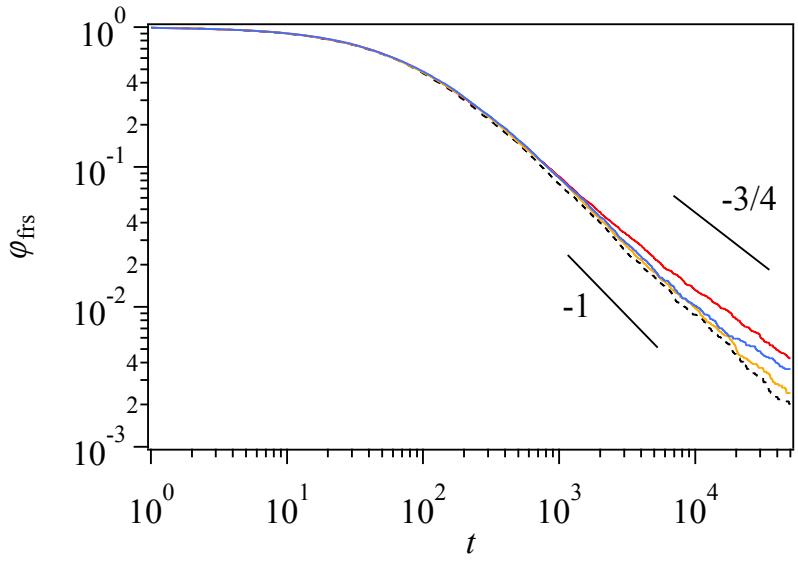

Figure 8 Time development of the fraction of free reaction sites $\varphi_{\rm frs}$ for various slip-spring densities. The density is converted to the average number of polymer segments between two anchoring points of slip-springs along the chain, $N_{\rm e}^{\rm ss}$, which was varied as 2.4 (red), 4.8 (blue), 9.6 (orange), and infinity (no entanglement). Solid lines show power-law decays with the exponent of -1 and -3/4.

Figure 8 shows $\varphi_{\rm frs}$ for various slip-spring densities, which is converted to the average number of polymer segments between two anchoring points of slip-springs along the chain $N_{\rm e}^{\rm ss}$. As expected, the deviation from the non-entangled case becomes smaller for larger $N_{\rm e}^{\rm ss}$ values (lower slip-spring densities), for which the onset time of the retardation becomes longer. Because some polymers have several entanglements due to fluctuations, the late stage of the reaction may be dominated by such well-entangled polymers even for the large $N_{\rm e}^{\rm ss}$ cases, although the statistics are not sufficient for further analysis.

DISCUSSION

Below, we discuss several characteristic time and length scales for polymers and consider how these scales are related to the gelation kinetics. Owing to the simulation results, in which the

slow reaction is observed after the consumption of free linkers, we assume that the polymers directly react with each other, in the following discussion.

Let us start from the time scales. For entangled polymer dynamics, three characteristic relaxation times play significant roles. Namely, the relaxation time of an entanglement segment, the Rouse relaxation time, and the longest relaxation time. The characteristic relaxation time of a subchain between entanglements (slip-springs) can be estimated from the average value of beads between two anchoring points along the chain, $N_{\mathrm{e}}^{\mathrm{ss}}$=2.7, as $\tau_{\mathrm{e}}^{\mathrm{ss}} = \zeta {N_{\mathrm{e}}^{\mathrm{ss}}}^2 a^2/3\pi^2 k_B T = 1.9 \times 10^{-1}$. The Rouse time can be given by $\tau_{\mathrm{R}} = \zeta {N_{\mathrm{P}}}^2 a^2/3\pi^2 k_B T = 1.3 \times 10^{1}$. The longest relaxation time determined from a simulation without linkers is $\tau_d = 5.5 \times 10^{1}$. For these time scales, we observe no characteristic behavior of the gelation kinetics, and thus, we conclude that these timescales seem not significant.

Let us move to the length scales. First, we consider the initial (pre-gel) stage, where the polymers essentially diffuse freely. For the reaction, a chain end has to diffuse in a distance $\xi_{\mathrm{end}}^{(0)}$ to find another chain end. Such a distance can be estimated from the density of the chain ends. In equilibrium, polymer chains behave as ideal non-interacting chains, and the initial chain end density is $\rho_{\mathrm{end}}^{(0)} = 2\rho/N_{\mathrm{P}}$, where ρ = 4 is the bead density. For the case of $N_{\mathrm{P}} = 20$, $\rho_{\mathrm{end}}^{(0)} = 0.4$. The characteristic distance between chain ends is then estimated as $\xi_{\mathrm{end}}^{(0)} \simeq \left[\rho_{\mathrm{end}}^{(0)}\right]^{-1/3} = 1.4$. The diffusion of chain ends would not be affected by the entanglement when $\xi_{\mathrm{end}}^{(0)}$ is not larger than the entanglement mesh size $\xi_{\mathrm{e}}^{\mathrm{ss}}$. The value of $\xi_{\mathrm{e}}^{\mathrm{ss}}$ in our simulation is $\xi_{\mathrm{e}}^{\mathrm{ss}} = \sqrt{N_{\mathrm{e}}^{\mathrm{ss}}}a = 1.5$, which is close to $\xi_{\mathrm{end}}^{(0)}$. At the initial stage, therefore, the gelation kinetics is hardly affected by the entanglements.

Second, we consider the late (post-gel) stage. At the late stage, the fraction of free reaction sites φ_{frs} decreases with time, and the chain end density decreases as $\rho_{\mathrm{end}} = \varphi_{\mathrm{frs}}\rho_{\mathrm{end}}^{(0)}$. Consequently, the characteristic distance between free reaction sites increases as $\xi_{\mathrm{end}} \simeq \rho_{\mathrm{end}}^{-1/3}$. Thus, when φ_{frs} becomes small, a chain end should diffuse a considerable distance to form a new cross-link. As we mentioned, at the late stage, entangled and cross-linked chains move via the arm retraction type

motion. Such a motion is dominant if ξ_{end} becomes comparable to the average end-to-end distance of a chain $\xi_{\mathrm{chain}} = \sqrt{N_{\mathrm{p}}}a = 4.5$. This condition corresponds to the free reaction site fraction of $\varphi_{\mathrm{frs}}^{*}$ $\simeq 1/\rho_{\mathrm{end}}^{(0)}\xi_{\mathrm{chain}}^{3} = 2.8 \times 10^{-2}$. Naively, for the time range that fulfills $\varphi_{\mathrm{frs}}(t) < \varphi_{\mathrm{frs}}^{*}$, the characteristic arm retraction time τ_{arm} is required for the systems with entanglements to form a new cross-link. On the other hand, without entanglements, the time necessary to create a new cross-link is essentially the Rouse time τ_{R}. Clearly, the arm retraction is much longer than the Rouse relaxation, $\tau_{\mathrm{arm}} \gg \tau_{\mathrm{R}}$. Thus, we conclude that the gelation kinetics is not sensitive to entanglements at the initial stage ($\varphi_{\mathrm{frs}} \simeq 1$) but is strongly affected by entanglements when $\varphi_{\mathrm{frs}} < \varphi_{\mathrm{frs}}^{*}$. This estimate is consistent with the simulation results.

CONCLUSIONS

To discuss the effect of entanglement on the reaction kinetics of gelation, we extended the MCSS model to the systems with end-link reactions and traced the time development of the system. The reaction kinetics is virtually insensitive to the inclusion of entanglement at the early stage of reaction before the network percolation, whereas it is delayed by the entanglement in the post-gel stage, in which all the linkers are connected to the polymers, yet free reactive sites remain. At the post-gel stage, time development of the number of unreacted sites obeys the power-law type decay with the exponent of -3/4. This behavior is consistent with the bead-spring simulations for dilute systems and the experimental result for UV curing of thiol-ene polymers. According to the analysis of the chain configurations, the retarded reaction is due to the dynamics of tethered polymers. Finally, it should be noted that the glassy contributions are not considered in the present modeling, and thus, some earlier results from simulations and experiments cannot be reproduced.

Appendix

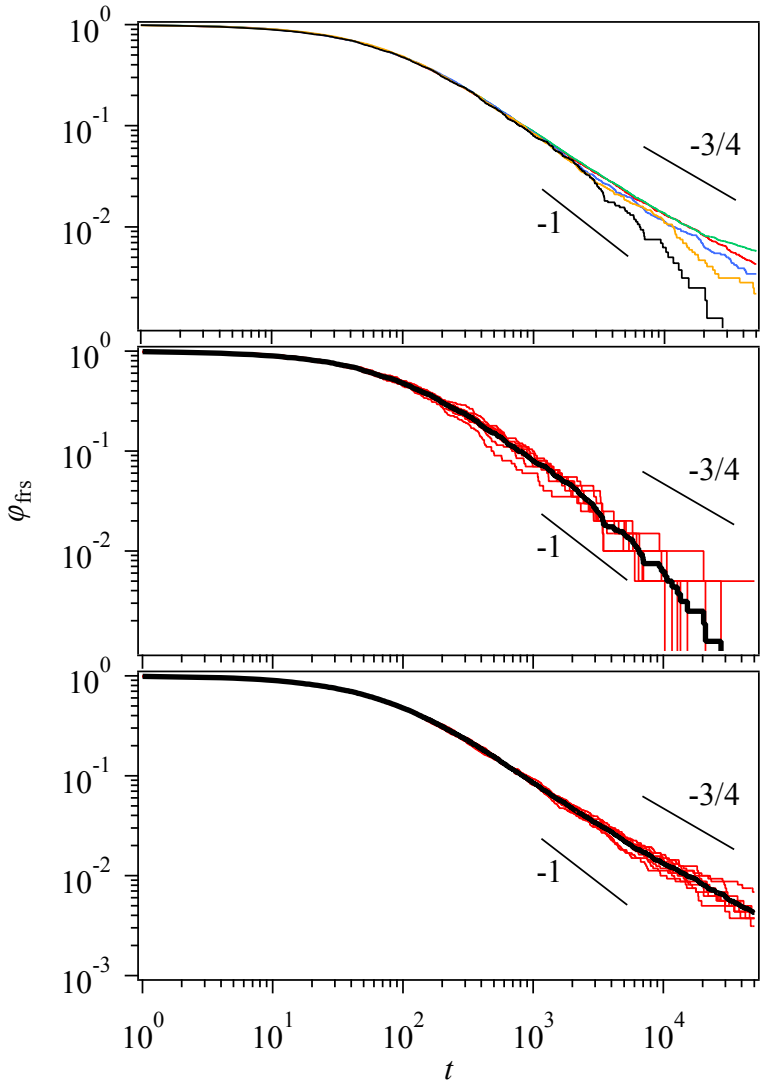

Figure 9 (Top) Time development of unreacted site numbers on linkers for various M_{p} chosen as 100 (black), 200 (orange), 400 (blue), 800 (red), and 1600 (green), respectively. (Middle and Bottom) Simulation trajectories in eight independent runs for $M_{\mathrm{p}} = 100$ (Middle) and $M_{\mathrm{p}} = 800$ (Bottom) with the averaged value (black). Solid lines show the power-law decays with the exponent of -1 and -3/4.

According to the nature of network formations under periodic boundary conditions, the system size has some effects on the results. Figure 9 top panel shows the time development of unreacted site fraction obtained with various system sizes. All the simulations were performed with slip-springs. For the smallest system, in which $M_{\mathrm{p}} = 100$ (black curve), the power-law exponent is close to unity,

and the retarded reaction is not seen. As shown in the middle panel, the rapid decay is not only due to the statistics but observed for each run. This fast decay in the small systems is due to a limited migration distance of the reaction sites. The effects of entanglement do not appear when the free dangling ends can find unreacted linker sites in their vicinity. For the large systems with $M_{\mathrm{p}} \geq 400$, the retardation in the reaction becomes obvious. For $M_{\mathrm{p}} = 800$, which was used for all the simulations discussed in the main text, the retarded reaction is fairly observed for all the trajectories as shown in the bottom panel, although the value of the power-law exponent is determined with an uncertainty. The result for the largest system with $M_{\mathrm{p}} = 1600$ (green curve) may hint further retardation around the end of the simulation, although the statistics are not enough.

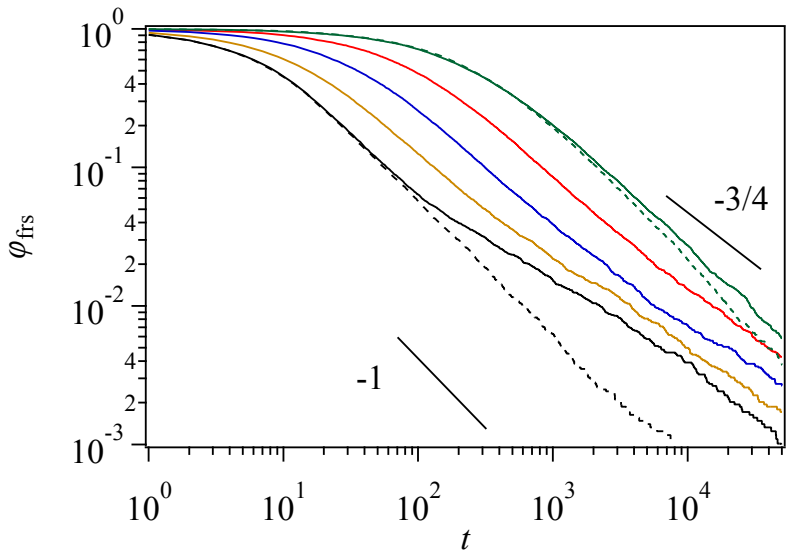

Figure 10 Time development of unreacted site numbers on linkers for various r_{r}^2 values varied as 2 (black), 1 (orange), 0.5 (blue), 0.25 (red), and 0.125 (green). The results without slip-springs are shown for $r_{\mathrm{r}}^2 = 2$ and 0.125 by broken curves. Solid lines show the power-law decays with the exponent of -1 and -3/4.

The kinetics of network formation is also affected by the reaction distance r_{r}. Figure 10 shows the time development of φ_{frs} with various r_{r}^2 values. As expected, the apparent reaction rate increases

with an increase in the r_r^2 value. For instance, in the pre-gel stage, the reaction with $r_r^2 = 2$ (black curve) proceeds faster ca. 30 times than that with $r_r^2 = 0.125$ (green curve). The retarded reaction due to the inclusion of slip-springs is observed for all the examined cases, but its appearance also depends on r_r^2. Namely, φ_{frs} exhibits a two-step decay with large r_r^2 values, and the shoulder becomes faint as r_r^2 decreases. The two-step decay is consistent with the scenario proposed in the main text. The fast process corresponds to the reaction dominated by the free diffusion, whereas the slow one reflects the arm-retraction type motion of the dangling chains. From this observation, we suggest that the power-law exponent larger than -1 appears in a transient time range between two reaction processes. Nevertheless, for numerical convenience, the simulations discussed in this paper were performed with $r_r^2 = 0.25$ ($r_r = 0.5$, shown by red curve) as mentioned in the main text.

Acknowledgments

This study is supported in part by Grant-in-Aid for Scientific Research (A) (17H01152) and for Scientific Research on Innovative Areas (18H04483) from JSPS. The support is also made by the Council for Science, Technology, and Innovation, Cross-ministerial Strategic Innovation Promotion Program, "Structural Materials for Innovation" from JST.

References

1 D. S. Achilias, *Macromol. Theory Simulations*, 2007, **16**, 319–347.

2 D. Toussaint and F. Wilczek, *J. Chem. Phys.*, 1983, **78**, 2642–2647.

3 K. Kang and S. Redner, *Phys. Rev. A*, 1985, **32**, 435–447.

4 E. Trommsdorff, H. Kohle and P. Lagally, *Makromolecular Chem.*, 1948, **1**, 169–198.

5 R. G. W. Norrish and R. R. Smith, *Nature*, 1942, **150**, 336–337.

6 B.-S. Chiou and S. A. Khan, *Macromolecules*, 1997, **30**, 7322–7328.

7 G. S. Grest, K. Kremer and E. R. Duering, *Epl*, 1992, **19**, 195–200.

8 W. Yang, D. Wei, X. Jin and Q. Liao, *Macromol. Theory Simulations*, 2007, **16**, 548–556.

9 M. Lang, A. John and J. U. Sommer, *Polymer (Guildf).*, 2016, **82**, 138–155.

10 C. Li and A. Strachan, *Polymer (Guildf).*, 2011, **52**, 2920–2928.

11 W. Y. Chiu, G. M. Carratt and D. S. Soong, *Macromolecules*, 1983, **16**, 348–357.

12 D. S. Achilias and C. Kiparissides, *Macromolecules*, 1992, **25**, 3739–3750.

13 L. H. Garcia-Rubio, M. G. Lord, J. F. MacGregor and A. E. Hamielec, *Polymer (Guildf).*, 1985, **26**, 2001–2013.

14 K. Dušek, *Polym. Gels Networks*, 1996, **4**, 383–404.

15 G. T. Russell, R. G. Gilbert and D. H. Napper, *Macromolecules*, 1992, **25**, 2459–2469.

16 G. T. Russell, *Macromol. Theory Simulations*, 1995, **4**, 549–576.

17 C. Barner-Kowollik and G. T. Russell, *Prog. Polym. Sci.*, 2009, **34**, 1211–1259.

18 M. Buback, M. Egorov and V. Kaminsky, *Macromol. Theory Simulations*, 1999, **8**, 520–528.

19 G. A. O'Neil, M. B. Wisnudel and J. M. Torkelson, *Macromolecules*, 1996, **29**, 7477–7490.

20 T. Uneyama and Y. Masubuchi, *J. Chem. Phys.*, 2012, **137**, 154902.

21 M. Langeloth, Y. Masubuchi, M. C. Böhm and F. Müller-plathe, *J. Chem. Phys.*, 2013, **138**, 104907.

22 Y. Masubuchi and T. Uneyama, *Soft Matter*, 2018, **14**, 5986–5994.

23 Y. Masubuchi, *Macromolecules*, 2018, **51**, 10184–10193.

24 K. Kremer and G. S. Grest, *J. Chem. Phys.*, 1990, **92**, 5057.

25 T. Okabe, Y. Oya, K. Tanabe, G. Kikugawa and K. Yoshioka, *Eur. Polym. J.*, 2016, **80**, 78–88.

26 G. Megariotis, G. G. Vogiatzis, A. P. Sgouros and D. N. Theodorou, *Polymers (Basel).*, , DOI:10.3390/polym10101156.

27 P. J. Flory, *J. Am. Chem. Soc.*, 1941, **63**, 3083–3090.

28 W. H. Stockmayer, *J. Chem. Phys.*, 1944, **12**, 125–131.

29 A. Izumi, Y. Shudo, K. Hagita and M. Shibayama, *Macromol. Theory Simulations*, 2018, **27**, 1700103.

30 D. S. Pearson and E. Helfand, *Macromolecules*, 1984, **17**, 888–895.

31 S. T. Milner and T. C. B. McLeish, *Macromolecules*, 1997, **30**, 2159–2166.

TOC graphic

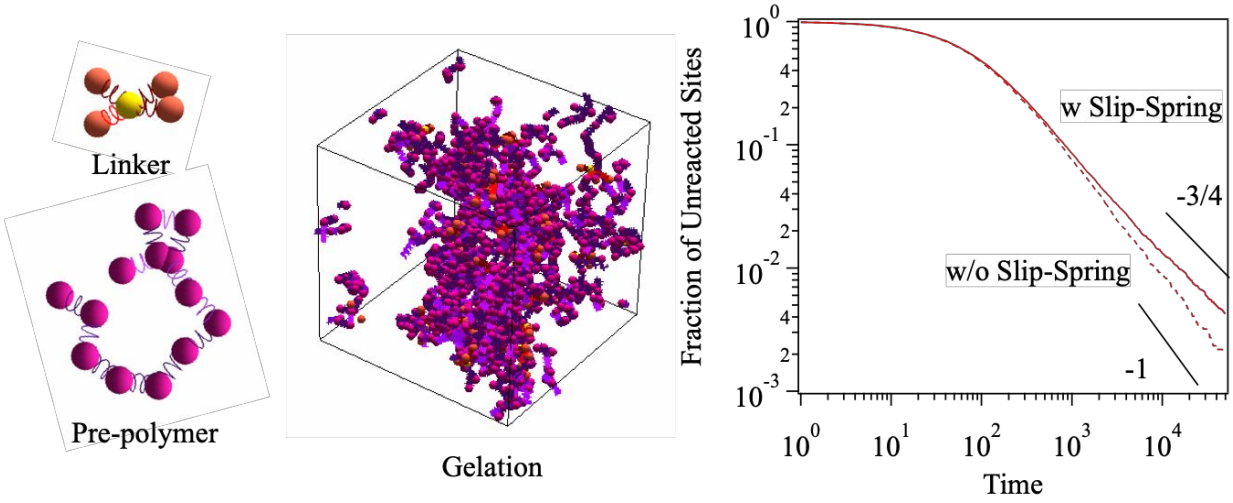

Entanglement affects gelation kinetics of polymers in the post-gel stage in multi-chain slip-spring simulations